DOI: 10.1021/bi900219c

BIOCHEMISTRY
including biophysical chemistry & molecular biology
Article

Cellular Membrane Disruption by Amyloid Fibrils Involved Intermolecular Disulfide Cross-Linking[†]

Bo Huang,[‡,∥] Jing He,[§,∥] Jing Ren,[‡] Xiang-Yang Yan,[‡] and Cheng-Ming Zeng*[,‡]

[‡]*College of Chemistry and Material Science, Shaanxi Normal University, Xi'an 710062, China, and* [§]*College of Life Science, Sihcuan University, Chengdu 610064, China* [∥] *These authors contributed equally to this work*

Received February 10, 2009; Revised Manuscript Received May 17, 2009

ABSTRACT: Accumulating evidence has strongly suggested that amyloid fibrils of protein or peptide are cytotoxic. Fibrillar species appear to lead to disruption of cell membrane structures and thereby cause cell death. In this study, human erythrocytes were used as an in vitro model to examine the disruptive effect of lysozyme fibrils on the plasma membrane. Both the protofibrils and mature fibrils induced hemolysis and aggregation of erythrocytes. Treating ghost membranes with the fibrils resulted in aggregation of membrane proteins through intermolecular disulfide cross-linking. LC−ESI-MS/MS and Western blotting analysis showed that lysozyme fragments were incorporated into the aggregates of ghost membrane proteins, which suggested that thio−disulfide exchange among lysozyme and membrane proteins was triggered when the fibrils interacted with erythrocyte membranes. Metal-ion chelators, radical scavengers, and antioxidants had no effect on the amyloid-induced disulfide cross-linking. The exposure of interior hydrophobic residues and the increased level of solvent-accessible disulfides in the lysozyme fibrils are thought to be involved in membrane disruption. These results may unveil a novel pathway for the cytotoxicity of amyloid fibrils.

More than 20 human diseases are associated with the conversion of polypeptides from their native state into highly ordered, β-sheet-enriched aggregates known as amyloid fibrils (*1*). The presence of these aggregates in the vicinity of dying cells and tissues led to the hypothesis that amyloid fibrils form and cause organ dysfunction due to the polypeptide accumulating and self-assembling into fibrillar forms on the cell membrane (*2*, *3*). Amyloid formation is a complex process and proceeds through a series of heterogeneous intermediates of various sizes and morphologies, including oligomers, protofilaments, and mature fibrils. Oligomers and protofilaments have been identified as the main species that are responsible for the cytotoxicity of amyloid fibrils (*4*), although in some cases, monomers, nonfibrillar or amorphous aggregates, and mature fibrils also exhibit cytotoxicity (*5*, *6*). The mechanism by which the fibrillar species of a protein induces cell damage has been studied extensively (*7*−*9*). Numerous observations have indicated that the primary interacting site of amyloid fibrils is the target cell membrane. As a consequence of fibril interaction, the structure and properties of the membrane are altered, and a cascade of events leading to cell death is triggered. Alteration of the membrane by amyloid fibrils includes channel or pore formation and enhancement of permeability (*2*, *3*), receptor activation (*10*), lipid loss (*11*), membrane fragmentation (*12*), and oxidation of membrane lipids and proteins (*13*, *14*).

A broad spectrum of proteins, including some nonpathogenic ones, has been demonstrated to be able to form amyloid fibrils. Fibril formation involves rearrangement of the hydrogen bonds and backbone of a protein, which can result in exposure of the hydrophobic interior and other reactive groups, e.g., disulfides, to the environment. These exposed domains promote amyloid fibrils to interact with lipid bilayers and to trigger oxidative stress, which leads to disruption of the cell membrane.

Human lysozyme with point mutations is related to non-neuropathic systemic amyloidosis (*15*). Its wild type can also form amyloid fibrils in vitro that are similar to those extracted from pathological deposits in tissue. Hen egg white lysozyme (termed lysozyme here) is a well-characterized protein and has been used as an alternative in vitro model for studying amyloidogenesis of proteins. Lysozyme is a small global protein with a single chain that consists of 129 amino acid residues and four disulfide linkages. Incubation of lysozyme under conditions of low pH and elevated temperatures results in the formation of amyloid fibrils (*16*). A recent experiment has shown that lysozyme fibrils reduce the viability of neuroblastoma cells through apoptotic and necrotic pathways (*17*).

In this study, human erythrocytes were used as a model to examine the disruptive effect of lysozyme fibrils on the cell membrane. The results showed that both the protofibrils and mature fibrils induced aggregation and hemolysis of erythrocytes. Incubating ghost membranes with fibrils resulted in co-aggregation of lysozyme and membrane proteins through intermolecular

[†]This work was supported by a grant from Shaanxi Normal University to C.-M.Z.

*To whom correspondence should be addressed: College of Chemistry and Material Science, Shaanxi Normal University, Xi'an 710062, China. Fax: +86 29 85307774. Telephone: +86 29 85303871. E-mail: chengmingz@hotmail.com.

 Published on Web 05/18/2009

sulfide cross-linking. The role of disulfides and free sulfhydryl groups in the interaction of lysozyme fibrils with ghost membranes was explored.

MATERIALS AND METHODS

Materials. Hen egg-white lysozyme (molecular mass of 14.3 kDa), dithiothreitol (DTT),[1] thioflavin T (ThT), monobromobimane (mBBR), 1-anilinonaphthalene 8-sulfonate (ANS), *N*-ethylmaleimide (NEM), phenylmethanesulfonyl fluoride, desferrioxamine, 5,5-dithiobis(2-nitrobenzoic acid) (DTNB), 2,6-di-*tert*-butyl-4-methylphenol (BHT), and quercetin were purchased from Sigma-Aldrich (St. Louis, MO). Sequencing-grade trypsin was purchased from Promega (Madison, WI). Electrophoresis-related reagents were from Promega and Amersham (Uppsala, Sweden). Other reagents were of analytical grade or HPLC grade. Fresh blood was drawn from healthy volunteers using sodium citrate as an anticoagulant.

Preparation and Characterization of Lysozyme Amyloid Fibrils. Lysozyme fibrils were prepared by incubating the protein (1.4 mM) in 10 mM HCl containing 0.02% NaN_3 at pH 2.0 and 65 °C for up to 10 days (*16*). The growth of lysozyme fibrils was monitored by ThT fluorescence and transmission electron microscopy (TEM). ThT fluorescence was measured in a mixture of 35 μM protein and 10 μM ThT, with excitation at 440 nm and emission at 482 nm in a Perkin-Elmer LS55 spectrofluorimeter. For TEM measurements, an aliquot of lysozyme fibrils was diluted 20-fold with water and dropped onto copper-mesh grids. Samples were negatively stained with 2% (w/v) uranyl acetate and air-dried at room temperature. Observations were made using a Hitachi H-600 electron microscope with an accelerating voltage of 80 kV.

Quantification of Free Sulfhydryl Groups and Disulfides. Quantification of free sulfhydryl groups of lysozyme fibrils and ghost membranes was performed according to Ellman's method (*18*). The DTT-accessible disulfides of native and fibrillar lysozyme were determined by the mBBR method (*19*) with modification. Briefly, lysozyme samples were added with 2 mM DTT and incubated at room temperature for 1 h. mBBR was then added from a stock solution in acetonitrile to a final concentration of 5 mM and incubated for 20 min. To the mixtures was added 30% trichloroacetic acid (TCA), and they were allowed to stand for 30 min in the dark. The samples were centrifuged at 15000*g*, and the pellets were washed with 1% TCA and centrifuged again. The pellets were dissolved in 100 mM Tris-HCl (pH 8.0) containing 1% SDS, and fluorescence was measured at 450 nm with excitation at 380 nm using a Perkin-Elmer LS-55 spectrofluorometer. Cysteine was used as a standard for calibration.

ANS Binding Assay. The emission spectra of ANS fluorescence in the presence of lysozyme fibrils were recorded between 400 and 600 nm using an excitation wavelength of 350 nm. Aliquots of the incubated mixture were diluted in phosphate buffer (50 mM, pH 7.0) containing 25 μM ANS. The ANS fluorescence was then scanned immediately, and the intensity at 465 nm was measured.

Ultracentrifugation of Lysozyme Fibrils. The fibrils were separated into three portions using a Hitachi CS150GXL microultracentrifuge. Fraction A consisted of the pellets collected by centrifugation of the mature fibrils at 50000*g* for 40 min. The supernatant was further centrifuged at 200000*g*. The pellets and the supernatant were named fraction B and fraction C, respectively. The pellets were resuspended in deionized water and stored at 4 °C until use. Protein was quantified by the Bradford assay (*20*) using native lysozyme as the standard.

Preparation of Erythrocytes and Ghost Membranes. Fresh blood was centrifuged at 1000*g* for 10 min, and erythrocytes were separated from plasma and buffy coat and washed three times with isotonic phosphate buffer [10 mM NaH_2PO_4/Na_2HPO_4, 5 mM KCl, and 140 mM NaCl (pH 7.4)]. The erythrocyte suspensions used in experiments were prepared daily. Erythrocyte ghost membranes were prepared by hypotonic hemolysis. Packed erythrocytes were lysed by diluting the cells in hypotonic phosphate buffer in the presence of phenylmethanesulfonyl fluoride. The lysates were centrifuged at 30000*g* for 20 min at 4 °C, and the pellets were resuspended and washed with phosphate buffer. Centrifugation and washing were repeated three times, and the final white pelleted ghost membranes were resuspended in the same buffer and stored at −40 °C.

Lysozyme Fibril-Induced Hemolysis. Erythrocyte suspensions (1% hematocrit) were incubated at 37 °C for 40 min in the presence of lysozyme fibrils. An aliquot of the reaction mixture was removed and centrifuged at 1000*g* for 10 min, with the absorbance of the supernatant determined at 540 nm. The control value (100% hemolysis) was determined using the same volume of erythrocyte diluted with water.

Scanning Electron Microscopy (SEM). Erythrocytes (1% hematocrit) were incubated for 40 min at 37 °C in the presence and absence of mature lysozyme fibrils. After incubation, the samples were centrifuged at 1000*g* for 10 min and the packed cells were resuspended in isotonic phosphate buffer that contained 1% glutaraldehyde. After fixation, samples were dehydrated through graded acetone, critical-point dried, and gold-coated by sputtering. The morphological changes in the erythrocytes were visualized with a Quanta 200 scanning electron microscope at an accelerating voltage of 20 kV.

Gel Electrophoresis of Ghost Membranes Treated with Amyloid Fibrils. SDS−PAGE was performed by using a 5% stacking gel and a 10% separating gel (2.6% C). Aliquots of ghost membranes were incubated at 37 °C for 40 min in the presence or absence of native lysozyme or fibrils. Some samples were treated in the presence of 10 mM DTT for disulfide reduction or 5 mM NEM for sulfhydryl blocking. Bands were visualized by Coomassie brilliant blue R-250 staining. For the Western blotting assay, the gel bands were transferred to a polyvinylidene fluoride membrane (0.45 μm, Millipore) with a mini transfer cell (GE Healthcare). The blots were probed with lysozyme antibody (Abcam, Cambridge, U.K.) and visualized by enhanced chemiluminescence (GE Healthcare).

In-Gel Digestion and Liquid Chromatography−Electrospray Ionization Tandem Mass Spectrometry (LC−ESI-MS/MS) Analysis of High-Molecular Mass Aggregates (HMWAs). The target bands were cut from the gel and washed with water and 50% (v/v) acetonitrile in 25 mM NH_4HCO_3 buffer until the color disappeared. The gel pieces were dried and reduced with 10 mM DTT. Alkylation was achieved via addition of 55 mM iodoacetamide and incubation in the dark for 45 min. In-gel trypsin digestion was conducted at 37 °C overnight.

[1]Abbreviations: Aβ, amyloid-β peptide; ANS, 1-anilinonaphthalene 8-sulfonate; DTT, dithiothreitol; BHT, 2,6-di-*tert*-butyl-4-methylphenol; HMWAs, high-molecular mass aggregates; LC−ESI-MS/MS, liquid chromatography−electrospray ionization tandem mass spectrometry; NEM, *N*-ethylmaleimide; SEM, scanning electron microscopy; TEM, transmission electron microscopy; ThT, thioflavin T.

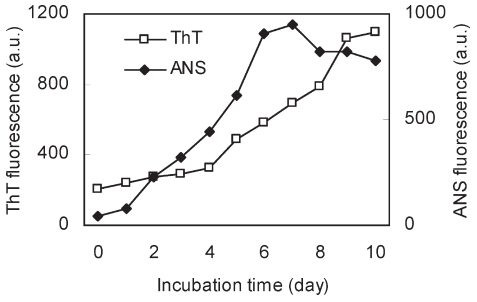

FIGURE 1: Kinetics of lysozyme fibril growth monitored by ThT and ANS fluorescence. Representative curves were derived from one of three independent incubations.

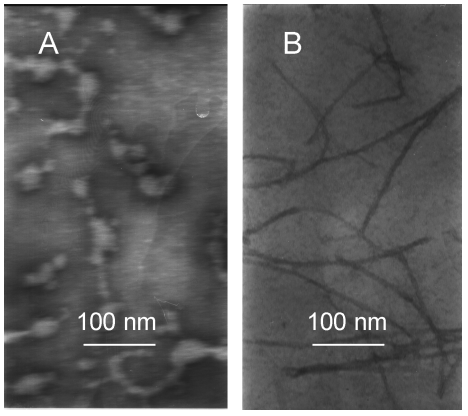

FIGURE 2: TEM images of lysozyme fibrils prepared under a single growth condition as described in Materials and Methods. The fibrils were 4 (A) and 10 days old (B). The 4-day-old aggregates demonstrate a beads-on-a-string morphology. Scale bars represent 100 nm.

Peptides were extracted and analyzed by LC−ESI-MS/MS on a Thermo Finnigan LTQ tandem mass spectrometer. Raw data were searched using the SEQUEST algorithm against the NCBI nonredundant database.

Statistical Analysis. Values are presented as means ± the standard deviation. A Student's paired *t* test was utilized to calculate the statistical significance.

RESULTS

Lysozyme Amyloid Fibril Formation and Characterization. The fibrillar species of lysozyme were obtained by incubating the protein (1.4 mM) at pH 2.0 and 65 °C. Mature lysozyme fibrils were harvested after incubation for 10 days. The ThT fluorescence assay showed that there was no obvious "lag phase" in the early stage of lysozyme fibrillation. Fibril growth was accelerated on the fourth day and reached a mature state in 9−10 days (Figure 1).

The intensity enhancement and blue shift of ANS fluorescence over the time course of the fibrillation process were also determined. The incubation of lysozyme resulted in a significant increase at 465 nm in ANS fluorescence (Figure 1), as well as a blue shift in the maximum wavelength, which reflected an increase in the solvent-exposed hydrophobic interior of the protein.

The morphology of the fibrillar species changed with incubation from amorphous granular aggregates to protofibrils and to mature fibrils with increasing binding affinities for ThT and ANS. On the fourth day of incubation, a so-called "beads-on-a-string" morphology (*21*) was observed via TEM (Figure 2A).

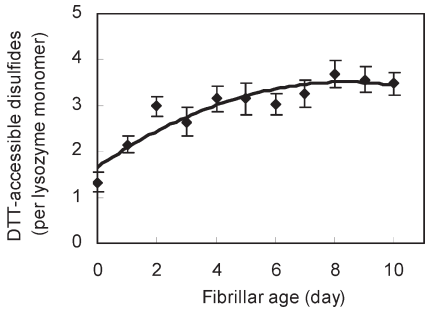

FIGURE 3: Solvent-accessible disulfide bonds of lysozyme in the duration of amyloid fibril growth. Disulfide data were calculated according to the free sulfhydryl groups formed by DTT reduction [means ± standard deviation (n = 5)].

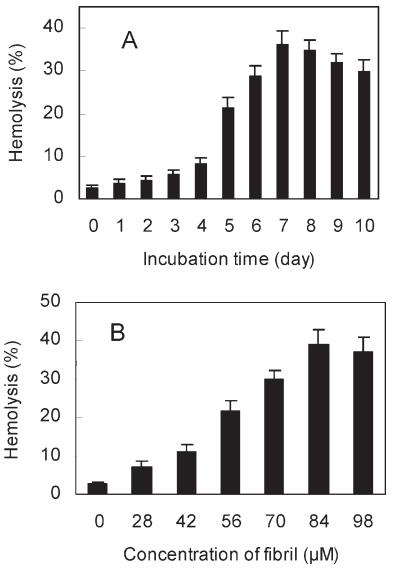

FIGURE 4: Hemolysis of erythrocytes induced by lysozyme fibrils. (A) Hemolysis of erythrocytes induced by lysozyme fibrillar species (70 μM) with differing amyloid ages. (B) Dose-dependent hemolysis induced by mature lysozyme fibrils. Erythrocyte suspensions (1% hematocrit) were incubated with the fibril species. Hemolysis is expressed as hemolytic rate against 100% lysis of erythrocytes. Experiments were performed in triplicate, and the results are shown as means ± the standard deviation.

The mature lysozyme fibril exhibited a typical morphology, characterized as long, straight, and partly twisted fibrils with diameters of 4−20 nm (Figure 2B).

The transformation of native lysozyme to amyloid fibril involves unfolding and reorganizing the polypeptide chains, in which more disulfide bonds became solvent-accessible (Figure 3). Quantification of free sulfhydryl groups of the fibrils was performed to exclude the possibility of free sulfhydryl formation during lysozyme fibrillation. No sulfhydryl group has been detected in the fibrillar species.

Hemolysis and Aggregation of Erythrocytes Induced by the Fibril Species of Lysozyme. Incubation of human erythrocytes in an isotonic environment with the fibril species of lysozyme resulted in hemolysis and cell aggregation. Both the protofibrils and mature fibrils induced hemolysis and aggregation of erythrocytes in an age-dependent (Figure 4A) and dose-dependent (Figure 4B) manner. The hemolytic effects increased with the growth of fibrils, and the 7-day-old fibrils exhibited maximum hemolysis data (Figure 4A). The subsequent decline in the hemolysis curve was partly caused by increased levels of

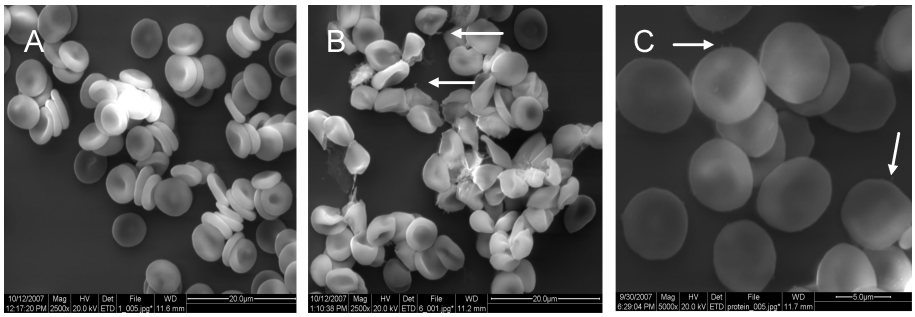

FIGURE 5: SEM imagines of erythrocytes after incubation in the presence or absence of lysozyme and mature lysozyme fibrils. (A) Control cells. (B) Cells incubated with 28 μM mature fibrils. The arrows indicate the fibril aggregates on the cell membrane. (C) Cells incubated with 28 μM native lysozyme. The arrows point to the lysozyme aggregates on the cell membranes. The scale bar represents 20 μm in panels A and B and 5 μm in panel C, as shown in the right corner of each image.

aggregation and deposition of hemoglobin, which led to lower absorbance at 540 nm. Therefore, the actual overall disruptive effect of the fibril species on erythrocytes, including hemolysis and cell aggregation, had a tendency to increase with fibril aging, in contrast to the previous view (*4*, *22*) that only oligomers and protofibrils exhibit cytotoxicity while mature fibrils show a weak or no effect.

Erythrocytes were prone to aggregation in the presence of mature fibrils. Aggregation of the cells occurred at a fibril concentration as low as 7 μM, at which hemolysis was not obvious. This phenomenon has also been observed recently by Chaudhary et al. (*23*), who found that extensive aggregation of erythrocytes and lipid vesicles was induced by a low dose of lysozyme fibrils.

SEM Studies of Morphological Alteration of Erythrocytes by Lysozyme Fibrils. Normally, erythrocytes have a biconcave discoid shape (Figure 5A), with high shape variability under physiological conditions. SEM images showed that cells incubated with 28 μM fibrils gathered into aggregates with deformed and broken shapes (Figure 5B). At higher concentrations of fibrils, the population of damaged and aggregated cells increased significantly. Numerous intact cells lost their biconcave shape and transformed mostly to stomatocytes and a few echinocytes, which indicated an increased difference between the tensions of the two leaflets of the cell membrane (*24*). As with its monomer, lysozyme fibrils are charged positively at physiological pH and, therefore, can be attracted to the anionic glycocalyx surface of the erythrocyte membrane. The electrostatic force drove the fibrillar species that accumulated on the membrane, which made the cells "sticky" toward each other and gathered into aggregates, as shown in Figure 5B. A small amount of amorphous aggregates was found on the membrane surface of erythrocytes treated with native lysozyme (Figure 5C), although these aggregates had no obvious effect on the permeability and morphology of the cell, which suggested that the fibrillar structure was a prerequisite for lysozyme to disrupt the intact cell membrane.

SDS−PAGE of Ghost Membranes Treated with Lysozyme Fibrils. The fibril-induced changes in the membrane protein pattern of erythrocytes have been assessed by gel electrophoresis of ghost membranes. The results indicated that lysozyme fibrils induced aggregation of ghost proteins. As shown in Figure 6A, the HMWAs of membrane proteins appeared on the top of the gel lanes and in the sample wells. At the same time, most of the other bands in the gel were weakened, except for band 7. Sulfhydryl blocking reagent NEM (5 mM) and reductant DTT (10 mM) inhibited significantly the effect of the fibrils on

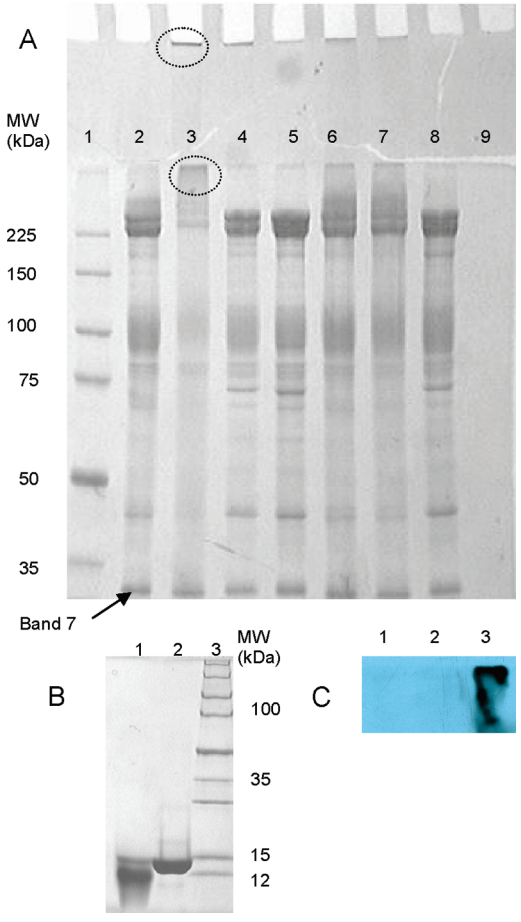

FIGURE 6: SDS−PAGE of erythrocyte membranes and lysozyme fibrils. (A) Membrane disruptions induced by native lysozyme and mature fibrils. Samples were subjected to electrophoresis on a 10% gel: lane 1, molecular mass markers; lane 2, control membranes; lanes 3−5, membranes treated with 35 μM lysozyme fibrils (3) and with 35 μM fibrils in the presence of 5 mM NEM (4) and 10 mM DTT (5), respectively; lanes 6−8, membranes treated with 35 (6) and 70 μM native lysozyme (7) and 70 μM lysozyme supplemented with 10 mM DTT (8), respectively; and lane 9, lysozyme fibrils (20 μg). The circled bands of lane 3 were sliced for MS analysis. (B) SDS−PAGE of native lysozyme and mature fibrils. Electrophoresis was performed on an 18% gel. Lanes 1−3 contained mature fibrils, native lysozyme, and molecular mass markers, respectively. (C) Western blotting results of ghost membranes (lane 1), lysozyme fibrils (lane 2), and membranes treated with 35 μM lysozyme fibrils (lane 3).

membrane proteins (lanes 4 and 5), suggesting that intermolecular disulfide cross-linking was involved in the aggregation of membrane proteins. However, NEM did not completely inhibit

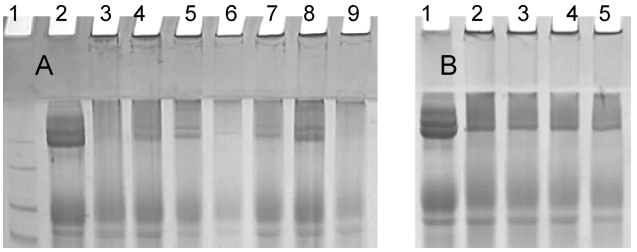

FIGURE 7: Effects of small molecules and fibrillar sizes on fibril-induced HMWAs. Fibrillar species corresponding to 35 μM lysozyme were applied in the samples. Samples were subjected to electrophoresis on a 10% gel. (A) Effects of metal-ion chelators, antioxidants, and free radical scavengers on fibril-induced HMWAs. Ghost membranes were mixed with the compounds prior to the fibril treatment: lane 1, molecular mass markers; lane 2, control membranes; lane 3, fibril-treated membranes; and lanes 4−9, membranes treated with the fibrils in the presence of 1 mM desferrioxamine (lane 4), 2 mM EDTA (lane 5), 5 mM ascorbic acid (lane 6), 2 mM BHT (lane 7), 1 mM quercetin (lane 8) and 10 mM mannitol (lane 9), respectively. (B) Effects of fibrillar sizes on fibril-induced HMWAs: lane 1, control membranes; lane 2, membranes and fibrils; lane 3, membranes and fraction A (the pellets at 50000*g*); lane 4, membranes and fraction B (the pellets at 200000*g*); and lane 5, membranes and fraction C (the supernatant at 200000*g*).

the disulfide cross-linking, as shown in lane 5, because of its inability to reduce the formed disulfides.

No aggregate was visualized in lane 9, to which mature fibrils were applied. Instead, SDS−PAGE with a high concentration of acrylamide (18%) and a Tricine buffer system showed that the fibrils could be separated into lysozyme monomers and small-size peptide fragments (Figure 6B), which indicated the absence of intermolecular disulfide cross-linkage in the fibrils.

Unexpectedly, lysozyme was also shown to promote aggregation of ghost proteins (lane 6 and 7), which was diminished by addition of DTT (lane 8) and NEM (data not shown). This may indicate that lysozyme monomers aggregated upon interacting with ghost membranes, and the resultant aggregates acted similarly to amyloid fibrils, to induce intermolecular disulfide cross-linking of membrane proteins. However, the disruptive effect of nonfibrillar lysozyme on ghost membranes was dose-independent and much weaker than that of the fibrillar form.

Metal-ion chelators desferrioxamine (1 mM) and EDTA (2 mM), antioxidants ascorbic acid (5 mM) and BHT (2 mM), and free radical scavengers mannitol (10 mM) and quercetin (1 mM) did not exhibit obvious protection of ghost proteins from fibril-induced aggregation (Figure 7A). This suggested that metal-catalyzed oxidation and free radicals were not involved in membrane disruption.

Hemolysis and HMWA Formation Induced by the Fibrillar Fractions. Mature amyloid fibrils have been characterized by high heterogeneity of species, containing long fibrils up to micrometers, and short fibrils, oligomers, and remaining monomers in sizes down to nanometers (*8*, *16*, *17*). To clarify the membrane-disruptive effects of lysozyme fibrillar species, mature amyloids were fractionated into three portions by ultracentrifugation. Fraction A consisted of the first pellets at 50000*g* and fraction B the second pellets at 200000*g*, and fraction C was the final supernatant. A quantitative assay showed that 31.0, 24.5, and 44.5% of the lysozyme were found in fractions A−C, respectively (Table 1). The values of DTT-accessible disulfides were similar in fractions A−C and mature fibrils; no significant difference was found (Table 1). As shown in Figure 7B, these three fractions had disruptive effects on ghost membranes similar

Table 1: Properties of the Fibrillar Species Fractionated by Ultracentrifugation

	fraction A	fraction B	fraction C	mature fibrils
protein content (%)	31.0	24.5	44.5	100
disulfides[a]	3.51 ± 0.28	3.67 ± 0.24	3.71 ± 0.23	3.46 ± 0.29
hemolytic rate (%)	21.7 ± 2.5[b]	27.4 ± 3.1	30.3 ± 2.0	28.9 ± 3.2

[a] DTT-accessible disulfides per lysozyme monomer. Data were calculated according to the free sulfhydryl groups formed by DTT reduction. [b] $p < 0.05$ to compare with fraction B, fraction C, and mature fibrils. Fibrillar species corresponding to 70 μM lysozyme were applied in the hemolysis assay.

to those of the mature fibrils, inducing strong aggregation of membrane proteins. Hemolytic data showed that fraction A had a weaker effect than fraction B, fraction C, and mature fibrils (Table 1), probably because more aggregation and deposition of hemoglobin were induced by the large fibrillar species. These facts implied that the membrane disruption by lysozyme fibrils was dependent on the fibrillar aging and probably also on the exposure of disulfide bonds, rather than the fibrillar form and particle size of lysozyme assemblies.

Western Blotting and LC−ESI-MS/MS Identification of Lysozyme Fragments in the HMWAs. To clarify whether lysozyme and its fragments co-aggregated and associated into HMWAs through intermolecular disulfide cross-linking, the gel bands of HMWAs were transferred onto a blotting membrane for antibody recognition. Lysozyme was identified in the HMWAs (Figure 6C). LC−ESI-MS/MS analysis of the trypsin-digested products of the HMWAs was also performed. Sequence matching of the MS/MS data showed that the HMWAs were mixtures of ghost membrane proteins and lysozyme fragments. Cytoskeletal proteins, including spectrins, ankyrin, band 3, and band 4.2 proteins, were the main components of HMWAs. Six lysozyme fragments were identified (Figure 8) with a sequence coverage of 47% and probability values (*P* value) from 9.87×10^{-6} to 3.33×10^{-16}. Both the circled aggregates in lane 3 of Figure 6A had the same composition of proteins.

Considering no free sulfhydryls were detected in the amyloid fibrils, the co-aggregation of lysozyme fragments with ghost proteins suggested that free sulfhydryl groups of lysozyme could be generated as a consequence of the fibrils interacting with ghost membranes, and subsequent intermolecular disulfide cross-linking was triggered and proceeded among lysozyme and membrane proteins. Interestingly, the total number of sulfhydryl groups in ghost membranes did not change after treatment with fibrils, implying that only thiol−disulfide exchange occurred in the fibril−membrane system.

DISCUSSION

Lysozyme belongs to the class of enzymes that lyse the cell walls of bacteria by specifically hydrolyzing the 1,4-β-D-linkage between *N*-acetylhexosamine residues. In addition, lysozyme can also exert its antimicrobial action through structural transition. The nonenzymatic antimicrobial activity is produced or enhanced by exposing the hydrophobic interior of the protein through irreversible denaturing by heating (*25*) and partial reduction with DTT (*26*). Moreover, the cationic and hydrophobic properties of lysozyme have been demonstrated to cause perturbation and fusion of biological membranes (*27*). Accordingly, lysozyme binding to cell membranes or vesicles can be

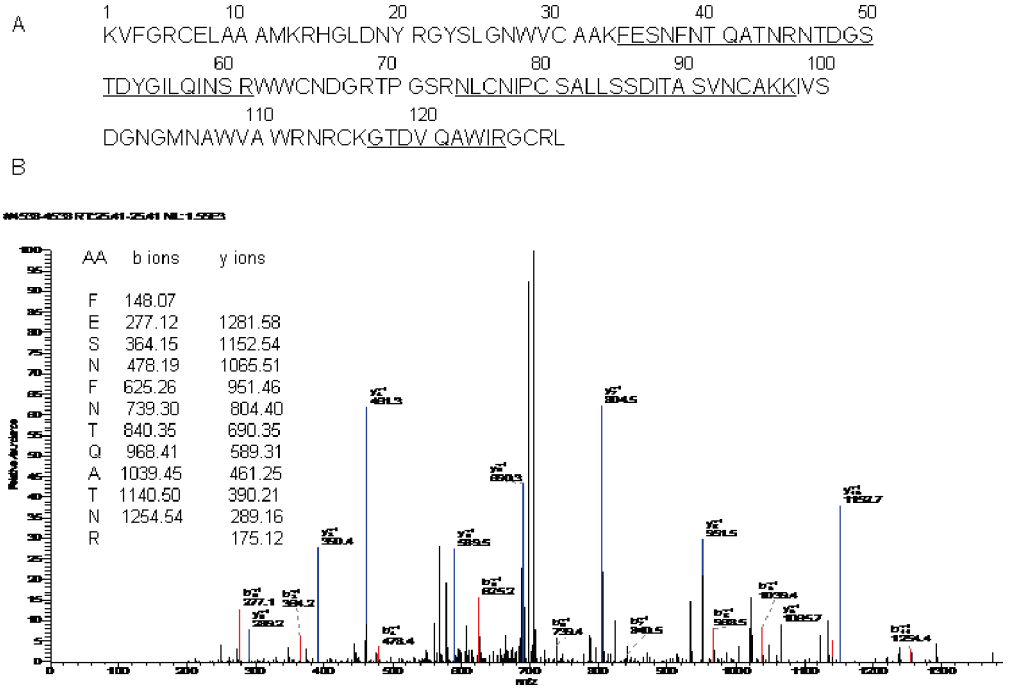

FIGURE 8: LC−ESI-MS/MS identification of lysozyme fragments in the HMWAs. (A) Amino acid sequence of hen egg white lysozyme. The underlined sequences were identified in the HMWAs by LC−ESI-MS/MS. (B) Tandem MS spectrum of the lysozyme fragment FESNFNTQATNR (residues 34−51) from an $[M + 2H]^{2+}$ ion at m/z 714.93. The y- and b-ions formed by peptide bond cleavage are shown in the inset.

accompanied by aggregation and subsequent penetration into lipid bilayers. In this study, aggregation of native lysozyme on the surface of erythrocyte membranes was visualized under SEM (Figure 5C). However, the binding of lysozyme did not result in obvious perturbation of the intact erythrocytes. In contrast, lysozyme induced the intermolecular disulfide cross-linking between ghost proteins, probably because the ghosts were deficient in cytosolic components such as hemoglobin and glutathione which serve to maintain the essential thiol−disulfide status of membrane proteins.

The conversion of lysozyme from its native form to amyloid fibrils increased significantly the disruptive effect of the protein on erythrocyte membranes. The hydrophobicity of the fibrillar species, probed by the fluorescent dye ANS, increased with the fibril aging and with the ability of the fibrils to induce hemolysis and aggregation of intact erythrocytes. This suggests that one of the pathways through which lysozyme fibrils disrupt the cell membrane is interaction between the hydrophobic domains of the protein and lipid bilayers.

Oxidative stress can be also a pathway of the amyloid fibril-induced cytotoxicity. Mounting evidence has shown that oxidative stress is a causal factor for triggering amyloid disorders (*28*−*30*). Amyloid fibrils and peptides such as amyloid-β peptide (Aβ) and its fragments have been found both in vivo and in vitro in association with the generation of radical oxygen species (ROS) (*31*). In turn, enhanced amyloid fibrillation of proteins under oxidized conditions has been observed (*32*). Oxidative stress can change the redox status of a cell and induce protein modification that leads to structural and functional alterations. In this study, however, metal-catalyzed oxidation and free radicals were not involved in the lysozyme fibril-induced intermolecular disulfide cross-linking. In addition, the total number of sulfhydryl groups in ghost membranes did not change after treatment with the fibrils. These facts probably suggest that oxidative stress is not a causal factor in the lysozyme fibril-induced membrane disruption. We propose that mixing the fibrils with ghost membranes changes the packing patterns of lipids and proteins and therefore makes the disulfides and free sulfhydryl groups of ghosts spatially more accessible to each other. Another driving force was derived from the disulfides in lysozyme fibrils. Upon unfolding and amyloid fibrillation, the disulfides of lysozyme become more solvent-accessible. The addition of fibrils to ghost membranes changed the SH/SS ratio, and therefore, the thiol−disulfide equilibrium was shifted. As a consequence, the redox potential of the disulfide−sulfhydryl couple can be altered, in favor of thiol−disulfide exchange between the free sulfhydryl groups and disulfides of membrane proteins and lysozyme. It has been reported (*33*) that, upon unfolding and at high pH, lysozyme monomers assembled into stable aggregates through a pathway of intermolecular disulfide cross-linking. However, more evidence is still required to elucidate precisely how the fibrils induce disulfide cross-linking between the proteins.

The reversible interchange of sulfhydryl groups and disulfide plays an important role in many biochemical pathways. Oxidation of the sulfhydryl groups or reduction of the disulfide bonds in a protein can result in activation or inactivation of protein functions (*34*). In this study, evidence that the disruptive impact of lysozyme fibrils on erythrocyte membranes is related to the fibril-induced intermolecular disulfide cross-linking of membrane proteins is provided. The disulfide cross-linking caused the aggregation or possibly the clustering of cytoskeletons and other membrane proteins which, in synergy with the hydrophobic effect of the fibril, could have led to enhancement of membrane permeability, cell aggregation, and breaking the cell into debris.

In conclusion, lysozyme can exert its disruptive effect on cellular membranes by exposing the hydrophobic interior of the protein (*25*, *26*). Our results demonstrate that transformation of native lysozyme to amyloid fibrils increased significantly the disruptive effect of the protein on erythrocyte membranes.

The hydrophobicity of the fibrillar species and the solvent-accessible disulfides is thought to be related to the ability of lysozyme fibrils to induce hemolysis and aggregation of intact erythrocytes. Treating ghost membranes with the fibrils resulted in co-aggregation of membrane proteins and lysozyme through intermolecular disulfide linking. The thiol−disulfide exchange among lysozyme and membrane proteins was triggered upon the fibrils interacting with erythrocyte membranes. Considering the recent report that Aβ fibrils promote disulfide bonding and aggregation of glyceraldehyde-3-phosphate dehydrogenase in cortical neurons (*35*), intermolecular disulfide cross-linking among proteins can be a general pathway in the amyloid fibril-induced cytotoxicity.

ACKNOWLEDGMENT

We are grateful to Jing Li for LC−ESI-MS/MS analysis and Professor Niels H. H. Heegaard for helpful discussions.

REFERENCES

(1) Dobson, C. M. (2003) Protein folding and misfolding. *Nature 426*, 884–890.
(2) Murphy, R. M. (2007) Kinetics of amyloid formation and membrane interaction with amyloidogenic proteins. *Biochim. Biophys. Acta 1768*, 1923–1934.
(3) Kagan, B. L., Hirakura, Y., Azimov, R., Azimova, R., and Lin, M. C. (2002) The channel hypothesis of Alzheimer's disease: Current status. *Peptides 23*, 1311–1315.
(4) Kayed, R., Head, E., Thompson, J. L., McIntire, T. M., Milton, S. C., Cotman, C. W., and Glabe, C. G. (2003) Common structure of soluble amyloid oligomers implies common mechanism of pathogenesis. *Science 300*, 486–489.
(5) Grudzielanek, S., Velkova, A., Shukla, A., Smirnovas, V., Tatarek-Nosso, M., Rehage, H., Kapurniotu, A., and Winter, R. (2007) Cytotoxicity of insulin within its self-assembly and amyloidogenic pathways. *J. Mol. Biol. 370*, 372–384.
(6) Sousa, M. M., Cardoso, I., Fernandes, R., Guimaraes, A., and Saraiva, M. J. (2001) Deposition of transthyretin in early stages of familial amyloidotic polyneuropathy: Evidence for toxicity of non-fibrillar aggregates. *Am. J. Pathol. 159*, 1993–2000.
(7) Gregersen, N., Bolund, L., and Bross, P. (2003) Protein misfolding, aggregation, and degradation in disease. *Methods Mol. Biol. 232*, 3–16.
(8) Bucciantini, M., Giannoni, E., Chiti, F., Baroni, F., Formigli, L., Zurdo, J. S., Taddie, N., Ramponi, G., Dobson, C. M., and Stefani, M. (2002) Inherent toxicity of aggregates implies a common mechanism for protein misfolding diseases. *Nature 416*, 507–511.
(9) Gorbenko, G. P., and Kinnunen, P. K. J. (2006) The role of lipid−protein interactions in amyloid-type protein fibril formation. *Chem. Phys. Lipids 141*, 72–82.
(10) Bamberger, M. E., Harris, M. E., McDonald, D. R., Husemann, J., and Landreth, G. E. (2003) A cell surface receptor complex for fibrillar β-amyloid mediates microglial activation. *J. Neurosci. 23*, 2665–2674.
(11) Sparr, E., Engel, M. F., Sakharov, D. V., Sprong, M., Jacobs, J., de Kruijff, B., Hoppener, J. W., and Killian, J. A. (2004) Islet amyloid polypeptide-induced membrane leakage involves uptake of lipids by forming amyloid fibers. *FEBS Lett. 577*, 117–120.
(12) Brender, J. R., Durr, U. H. N., Heyl, D., Budarapu, M. B., and Ramamoorthy, A. (2007) Membrane fragmentation by an amyloidogenic fragment of human Islet Amyloid Polypeptide detected by solid-state NMR spectroscopy of membrane nanotubes. *Biochim. Biophys. Acta 1768*, 2026–2029.
(13) Smith, D. G., Cappai, R., and Barnham, K. J. (2007) The redox chemistry of the Alzheimer's disease amyloid β peptide. *Biochim. Biophys. Acta 1768*, 1976–1990.
(14) Butterfield, D. A., and Lauderback, C. M. (2002) Lipid peroxidation and protein oxidation in Alzheimer's disease brain: Potential causes and consequences involving amyloid β-peptide-associated free radical oxidative stress. *Free Radical Biol. Med. 32*, 1050–1060.
(15) Pepys, M. B., Hawkins, P. N., Booth, D. R., Vigushin, D. M., Tennent, G. A., Soutar, A. K., Totty, N., Nguyen, O., Blake, C. C. F., Terry, C. J., Feest, T. G., Zalin, A. M., and Hsuan, J. J. (1993) Human lysozyme gene mutations cause hereditary systemic amyloidosis. *Nature 363*, 553–557.
(16) Frare, E., deLaureto, P. P., Zurdo, J., Dobson, C. M., and Fontana, A. (2004) A highly amyloidogenic region of hen lysozyme. *J. Mol. Biol. 340*, 1153–1165.
(17) Gharibyan, A. L., Zamotin, V., Yanamandra, K., Moskaleval, O. S., Margulis, B. A., Kostanyan, I. A., and Morozova-Roche, L. A. (2007) Lysozyme amyloid oligomers and fibrils induce cellular death via different apoptotic/necrotic pathways. *J. Mol. Biol. 365*, 1337–1349.
(18) Ellman, G. L. (1959) Tissue sulfhydryl groups. *Arch. Biochem. Biophys. 82*, 70–77.
(19) Krimm, I., Lemaire, S., Ruelland, E., Miginiac-Maslow, M., Jaquot, J. P., Hirasawa, M., Knaff, D. B., and Lancelin, J. M. (1998) The single mutation Trp35→Ala in the 35−40 redox site of *Chlamydomonas reinhardtii* thioredoxin *h* affects its biochemical activity and the pH dependence of C36-C39 ^{1}H-^{13}C NMR. *Eur. J. Biochem. 255*, 185–195.
(20) da Silva, M. A., and Arruda, M. A. (2006) Mechanization of the Bradford reaction for the spectrophotometric determination of total proteins. *Anal. Biochem. 351*, 155–157.
(21) Bitan, G., Kirkitadze, M. D., Lomakin, A., Vollers, S. S., Benedek, G. B., and Teplow, D. B. (2003) Amyloid β-protein (Aβ) assembly: Aβ40 and Aβ42 oligomerize through distinct pathways. *Proc. Natl. Acad. Sci. U.S.A. 100*, 330–335.
(22) Caughey, B., and Lansbury, P. T. (2003) Protofibrils, pores, fibrils, and neurodegeneration: Separating the responsible protein aggregates from the innocent bystanders. *Annu. Rev. Neurosci. 26*, 267–298.
(23) Chaudhary, N., and Nagaraj, R. (2009) Hen lysozyme amyloid fibrils induce aggregation of erythrocytes and lipid vesicles. *Mol. Cell. Biochem.* DOI 10.1007/s11010-009-0091-8.
(24) Tachev, K. D., Danov, K. D., and Kralchevsky, P. A. (2004) On the mechanism of stomatocyte-echinocyte transformations of red blood cells: Experiment and theoretical model. *Colloids Surf., B 34*, 123–140.
(25) Ibrahim, H. R., Higashiguchi, S., Juneja, L. R., Kim, M., and Yamamoto, T. A. (1996) Structural phase of heat-denatured lysozyme with novel antimicrobial action. *J. Agric. Food Chem. 44*, 1416–1423.
(26) Touch, V., Hayakawa, S., and Saitoh, K. (2004) Relationships between conformational changes and antimicrobial activity of lysozyme upon reduction of its disulfide bonds. *Food Chem. 84*, 421–428.
(27) Gorbenko, G. P., Ioffe, V. M., and Kinnunen, P. K. (2007) Binding of lysozyme to phospholipid bilayers: Evidence for protein aggregation upon membrane association. *Biophys. J. 93*, 140–153.
(28) Su, B., Wang, X., Nunomura, A., Moreira, P. I., Lee, H. G., Perry, G., Smith, M. A., and Zhu, X. (2008) Oxidative stress signaling in Alzheimer's disease. *Curr. Alzheimer Res. 5*, 525–532.
(29) Allsop, D., Mayes, J., Moore, S., Masad, A., and Tabner, B. J. (2008) Metal-dependent generation of reactive oxygen species from amyloid proteins implicated in neurodegenerative disease. *Biochem. Soc. Trans. 36*, 1293–1298.
(30) Butterfield, D. A., and Sultana, R. (2007) Redox proteomics identification of oxidatively modified brain proteins in Alzheimer's disease and mild cognitive impairment: Insights into the progression of this dementing disorder. *J. Alzheimer's Dis. 12*, 61–72.
(31) Murray, I. V., Sindoni, M. E., and Axelsen, P. H. (2005) Promotion of oxidative lipid membrane damage by amyloid β proteins. *Biochemistry 44*, 12606–12613.
(32) Giasson, B. I., Ischiropoulos, H., Lee, V. M., and Trojanowski, J. Q. (2002) The relationship between oxidative/nitrative stress and pathological inclusions in Alzheimer's and Parkinson's diseases. *Free Radical Biol. Med. 32*, 1264–1275.
(33) Kumar, S., Ravi, V. K., and Swaminathan, R. (2008) How do surfactants and DTT affect the size, dynamics, activity and growth of soluble lysozyme aggregates?. *Biochem. J. 415*, 275–288.
(34) Sevier, C. S., and Kaiser, C. A. (2002) Formation and transfer of disulphide bonds in living cells. *Nat. Rev. Mol. Cell Biol. 3*, 836–847.
(35) Cumming, R. C., and Schubert, D. (2005) Amyloid-β induces disulfide bonding and aggregation of GAPDH in Alzheimer's disease. *FASEB J. 19*, 2060–2072.